Communication in Physical Sciences, 2024, 11(3): 548-562

Computational Study of the Reaction Mechanism for the Formation of 4,5-Diaminophthalonitrile from 4,5-Dibromo-1,2-Diaminobenzene and Copper Cyanide

Kayode Sanusi

Received: 02 April 2024/Accepted: 20 June 2024/Published: 30 June 2024

Abstract: *This study investigates the mechanism of the reaction between 4,5-dibromo-1,2-diaminobenzene and copper cyanide using Density Functional Theory (DFT) calculations. The kinetics and the thermodynamic properties of the reaction were analyzed, revealing two major steps with activated complexes AC1 and AC2. Scheme 3 accurately depicts the reaction pathway. A triangular Cu-C=N moiety was found in the calculated transition states (TS), AC1 and AC2. The thermodynamic parameters for the first step show* ΔG *= -606.8 kJ mol*$^{-1}$ *,* ΔH *= -610.7 kJ mol*$^{-1}$ *and* ΔS *= -0.0132 kJ mol*$^{-1}$*K*$^{-1}$ *while for the second step* ΔG *= -600.1 kJ mol*$^{-1}$*,* ΔH *= -603.6 kJ mol*$^{-1}$*, and* ΔS *= -0.0117 kJ mol*$^{-1}$*K*$^{-1}$ *were obtained. The activation energies (*E_a *and* E_c*) for steps 1 and 2 are 189.0 kJ mol*$^{-1}$ *and 210.6 kJ mol*$^{-1}$*, respectively. The positive values of* $\Delta G^{\#}$ *and* $\Delta H^{\#}$ *confirm the presence of energy barriers in both steps.These findings provide critical insights into the energetics and mechanism of the DDB reaction with copper cyanide, which is very crucial in understanding the strategy for the development of efficient synthetic procedures for the phthalonitrile.*

Keywords: *Transition state, density functional theory, thermodynamic property, activation* barrier

Kayode Sanusi
Department of Chemistry, Obafemi Awolowo University, Ile-Ife, Nigeria
E-mail address: sosanusi@oauife.edu.ng
Orcid id: 0000-0003-0358-8666

1.0 Introduction

There exists a rather extensive literature on the syntheses and applications of metallophthalocyanines (MPcs) (Tunç *et al*., 2019; Yang *et al*., 2021; Lo *et al*., 2020; Gamelas *et al*., 2023; Gregory, 2000; Sanusi *et al*., 2014). The photophysical and photochemical behaviour of these macrocycles with or without covalently linked nanomaterials and their applications in many advanced technological fields have been extensively investigated (Tayfuroğlu *et al*., 2018; Korkmaz *et al*., 2020; Kahriman *et al*., 2020; Guney and Gorduk, 2023; Demirbaş, 2020; Yüzeroğlu *et al*., 2021; Harmandar *et al*., 2021; Aftab *et al*., 2022; Farajzadeh *et al*., 2022; Matlou and Nyokong, 2020; Albayrak *et al*., 2023; Ndebele and Nyokong, 2023; Madhuri and John, 2022; Baran *et al*., 2020). Their characteristic features such as intense absorption in the visible and near-IR spectral regions, and fluorescence properties, position them as important candidates for applications involving light scavenging, storage, control, and transmission (Sanusi *et al*., 2014). Their structural semblance to porphyrin, which is an important light scavenger in plants during photosynthesis underscores their significance in light-dependent applications. The relative ease of synthesis, purification, and modification of MPc structures, in addition to their interesting optical properties, make them compounds of choice for most advanced technological applications (Harmandar *et al*., 2021; Aftab *et al*., 2022; Farajzadeh *et al*., 2022; Matlou and Nyokong, 2020; Albayrak *et al*., 2023; Ndebele and Nyokong, 2023; Madhuri and John, 2022; Baran *et al*., 2020). It is therefore not surprising that the molecule is one of the most extensively studied aromatic compounds. The properties of MPcs required for most advanced applications have been

found to be enhanced when the molecules are linked to nanomaterials (Harmandar *et al*., 2021; Aftab *et al*., 2022; Farajzadeh *et al*., 2022; Matlou and Nyokong, 2020; Albayrak *et al*., 2023; Ndebele and Nyokong, 2023; Madhuri and John, 2022; Baran *et al*., 2020). This implies that by increasing the number of nanomaterials attached to phthalocyanine (Pc) molecules, the properties of the MPcs needed for most of the advanced technological applications would be enhanced. Currently, the maximum number of substitutable amine groups that are directly attached to the indoline units of the Pc are four. The amine substituents are by default limited to four by the most available synthetic methods for amino-substituted Pc derivatives (Zhang and Xu, 1994). These amino substituent groups are often the ones used for covalent linkage with nanomaterials. They are readily prepared by the reduction of the four -NO_2 groups of the tetranitro-phthalocyanine to amine (Fig. 1). The tetranitrophthalocyanines are formed by cyclization reaction of either 4-nitro- or 3-nitro phthalonitrile/phthalic anhydride to yield the corresponding tetranitroPcs (β-tetranitro or α-tetranitro) (Zhang *et al*., 2009), which in turn are reduced to tetraaminoPcs according to Fig. 1. There is no literature report on the preparation of 4,5-dinitrophthalonitrile yet to the best of our knowledge, otherwise, this same technique could have been used to prepare octa-substituted amino Pcs.

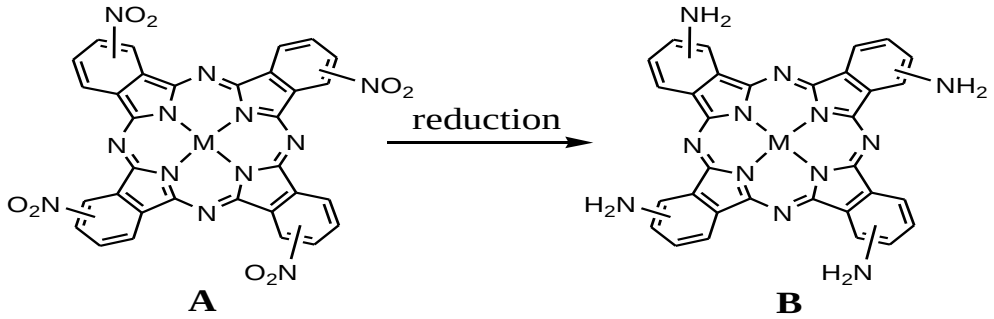

Fig. 1: Preparation of tetraaminopthalocyanines from tetranitrophthalocyanines

The four amine points of attachment in MPcs appear rather insufficient to give optimum results when these molecules are applied in most of the advanced technological fields. For example, in photodynamic therapy (PDT) of cancer, where photon energy is used to activate a photosensitizer (an MPc) to catalyze the conversion of ground-state molecular oxygen ($^3O_2$) to singlet oxygen ($^1O_2$) which ultimately is responsible for cancer cell death, the MPc-nanomaterial dyads are required to penetrate the porous diseased cell for enhanced drug delivery (Zi *et al*., 2022; Subhan *et al*., 2023; Camerin *et al*., 2010). This is referred to as the enhanced permeability and retention (EPR) effect (Zi *et al*., 2022; Subhan *et al*., 2023; Camerin *et al*., 2010). The EPR effect intensifies the drug-cancer cell interaction, the degree of which is lower when only the photosensitizer (drug) is administered without nanoparticles (Zi *et al*., 2022; Subhan *et al*., 2023; Camerin *et al*., 2010). A maximum of eight amine-substituent groups may be considered critical for a successful EPR effect since this is expected to increase the number of attachment points, and subsequently the number of nanoparticles that can be attached to the Pc molecule. The limitation to increasing the number of attachment points is caused by a lack of yet feasible synthetic procedure for an octa-substituted amino-Pc, Fig. 2. Apart from EPR effect, other areas of applications where octa-substituted amino-Pc is of immense value

include optical limiting (Sanusi *et al*., 2015), fluorescence sensing and imaging (Gvozdev *et al*., 2022; Adegoke and Nyokong, 2014; Idowu and Nyokong, 2012), photocatalysis (Kumar *et al*., 2019; Farahmand *et al*., 2023), photodegradation of pollutants (Pan *et al*., 2023), and photodynamic antimicrobial chemotherapy where silver nanoparticles are covalently attached to Pc molecules for enhanced antimicrobial property (Mafukidze *et al*., 2019; de Oliveira de Siqueira *et al*., 2022).

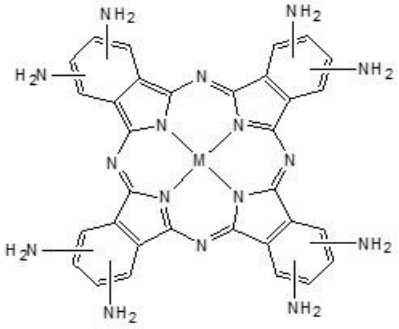

Fig. 2: **Octa-substituted amino-Pc**

Research effort towards increasing the number of amine functional groups around the Pc core from the default four is still, to the best of our knowledge, scarce – perhaps due to the notion that amine-phthalonitriles are prone to polymerization reaction because of the highly reactive amine group (Yüksel *et al*., 2008). There is currently no available synthetic method to produce 4,5-diaminophthalonitrile (DPN) directly. What is currently known is the formation of a protected -NH_2-phthalonitrile (Yüksel *et al*., 2005). The protected -NH_2-phthalonitrile was formed by nucleophilic substitution, where the two Br atoms in 4,5-dibromo-*N,N'*-ditosyl-*o*-phenylenediamine are displaced by the CN^- in CuCN using DMF as solvent (Yüksel *et al*., 2005) (Fig. 3).

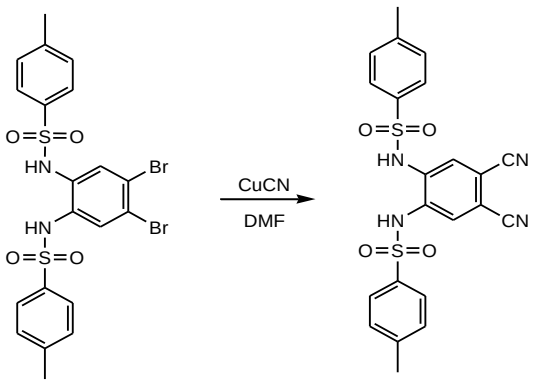

4,5-Dibromo-N,N'-ditosyl
-o-phenylenediamine

Fig. 3: Conversion of a protected amine-dibromobenzene (4,5-Dibromo-*N,N'*-ditosyl-*o*-phenylenediamine) to a protected amine-phthalonitrile (Yüksel *et al*., 2005)**.**

The formation of 4,5-diaminophthalonitrile (DPN) directly from 4,5-dibromo-1,2-diaminobenzene (DDB) and CuCN may be possible (as shown in Scheme 1) at room temperature without having to protect the -NH_2 group. Also, the tradition of protecting the amine groups of diaminophthalonitrile before forming the Pc may not be necessary (Yüksel *et al*., 2008; Yüksel *et al*., 2005), since no evidence shows amine-phthalonitrile cannot be cyclized without undergoing polymerization (Sanusi *et al*., 2014; Sanusi *et al*., 2014; Sanusi and Nyokong, 2014). The conditions under which an *o*-diaminobenzene or *m*-diaminobenzene would polymerize are quite different from those required for cyclization (Sayyah et al., 2014; Sánchez and Rivas, 2002).

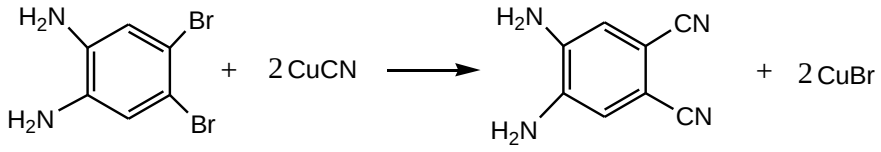

Scheme 1: Formation of 4,5-diaminophthalonitrile (DPN) from 4,5-dibromo-1,2-diaminobenzene (DDB)

2. 0 Theoretical and computational details

2.1. Consideration of possible reaction mechanisms

Based on the target reaction shown in Scheme 1, two different reaction schemes (2A and 2B) were proposed as follows:

A

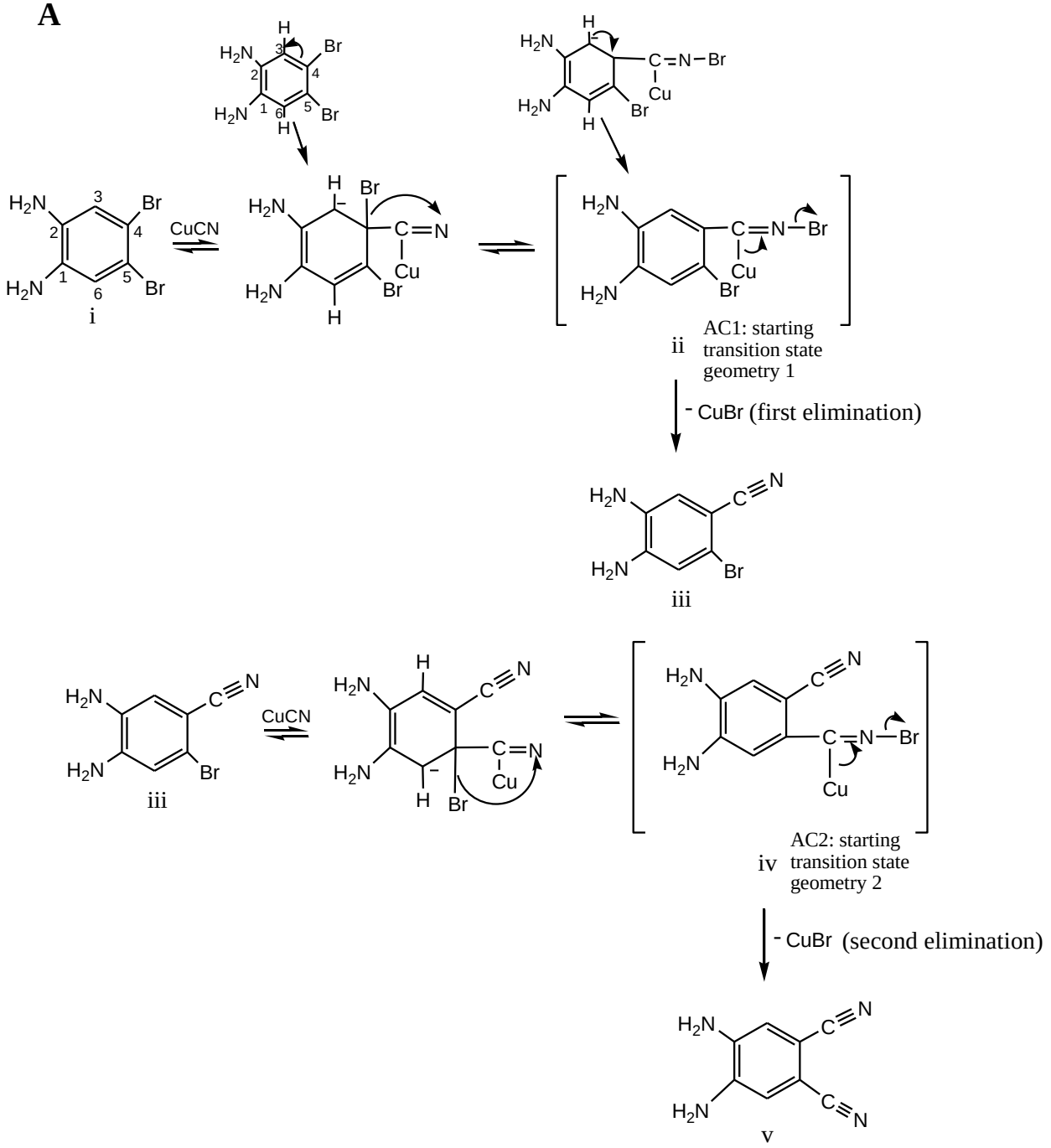

B

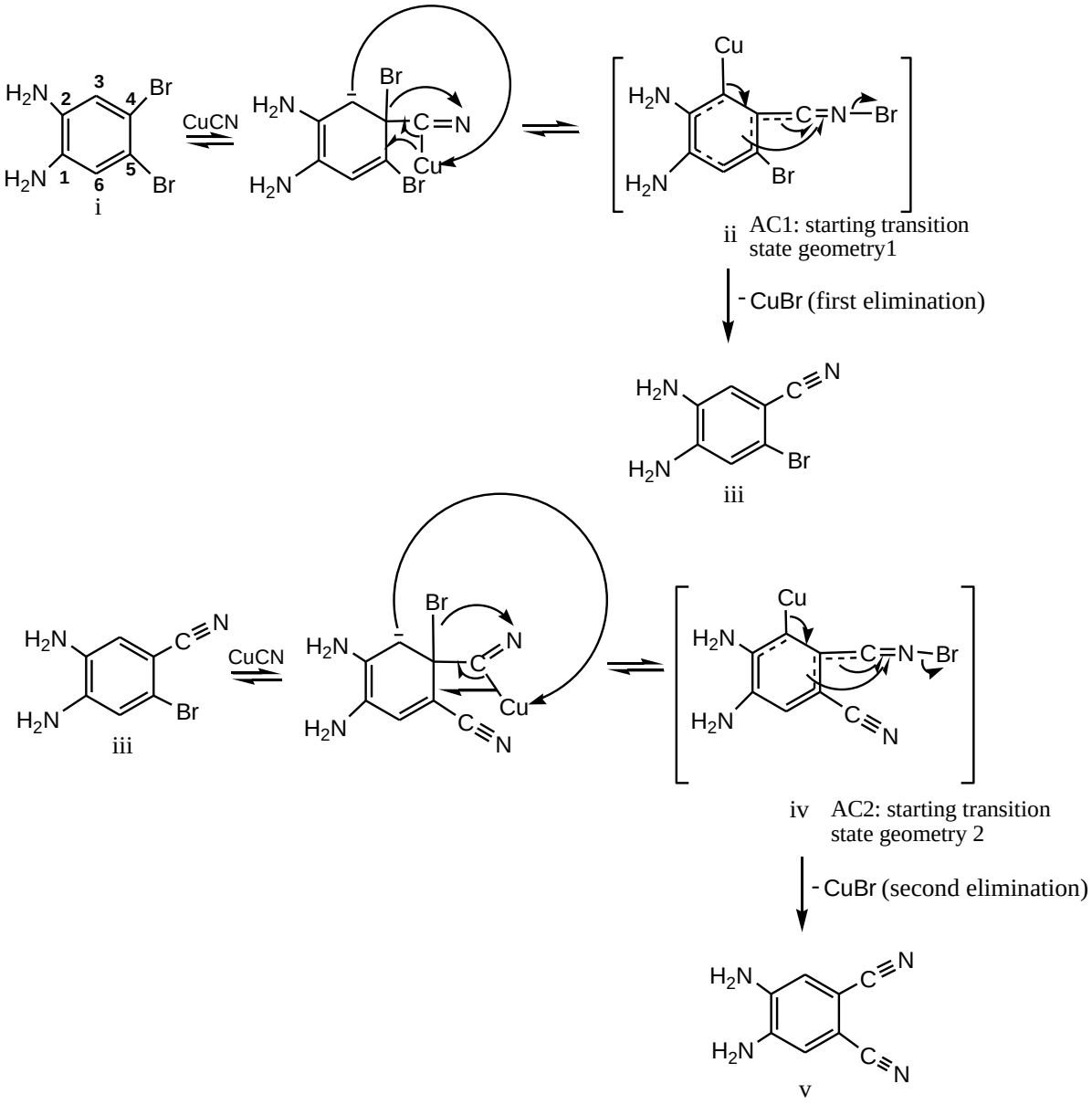

Scheme 2: Proposed reaction mechanisms (A and B) prior to DFT calculations.

2.2. Computational methodology

According to the proposed schemes (2A and 2B), DDB (i), 4,5-diamino-2-bromobenzonitrile DBN (iii), the two activated complexes (ii & iv) and DPN (v), were optimized employing the B3LYP functional (Song and Ma, 2010; Siddle *et al*., 2007; El-Azhary and Suter, 1996; Salzner, 2010) and 6-31G(D) basis set (Vijay *et al*., 2013; Mazzone *et al*., 2016). The optimization and frequency data of CuCN and CuBr were obtained at mPW1PW91/6-31G(D) level after careful benchmarking using three different methods, namely – mPW1PW91/6-31G(D), mPW1PW91/6-31G(D)/GENECP(SDD) and mPW1PW91/6-31G(D)/GENECP (LANL2DZ) with CuCN as the specimen (Figs. S1 – S3). These Figs., S1, S2 and S3, represent the results obtained from using mPW1PW91/6-31G(D), mPW1PW91/6-

31G(D)/GENECP(SDD) and mPW1PW91/6-31G(D)/GENECP (LANL2DZ) methods, respectively. Note that both mPW1PW91/6-31G(D)/GENECP(SDD) and mPW1PW91/6-31G(D)/GENECP (LANL2DZ) are mixed basis sets methods, where the 6-31G(D) in each case describes the properties of C and N atoms, and the SDD or LANL2DZ describes the properties of Cu atom (Sanusi *et al*., 2020). Calculation and analysis of the frequency of all the ground state structures ensured that their optimized structures correspond to the energy minima on the potential energy surface (PES), as evidenced by their zero imaginary frequency value (Figs. S1 – S7). The two activated complexes (ii and iv in scheme 3) were optimized to transition states (TS) using the TS Berny method (Suleimanov and Green, 2015) (Figs. S8 and S9). They are confirmed as true

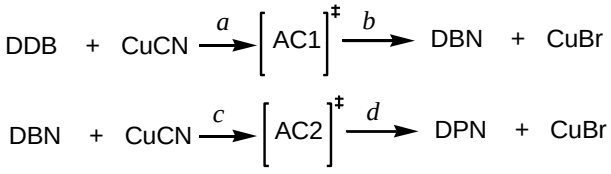

Note that equations 1 and 2 represent steps 1 and 2 of the overall reaction, respectively. The rate of the reaction may be predicted using the activation energy (E_A) calculated for the steps leading to the formation of AC1 and AC2.

The E_A and the thermodynamic properties of the relevant steps were calculated according to the following relationships:

$$E_A = E_{AC} - \sum E_R \quad (3)$$

$$\Delta G = \sum G_P - \sum G_R \quad (4)$$

$$\Delta H = \sum H_P - \sum H_R \quad (5)$$

$$\Delta S = \sum S_P - \sum S_R \quad (6)$$

where E_{AC}, E_R, G_P, G_R, H_P, H_R, S_R, S_P are the total energy of the activated complexes, total energy of the reactants, free energy of the products, free energy of the reactants, enthalpy of the products, enthalpy of the reactants, entropy of the products, and entropy of the reactants, respectively. The G for each chemical component of the reaction was obtained according to Eq. 7:

TS state structures by the resulting single imaginary (negative) frequency obtained from the frequency calculations. Intrinsic reaction coordinate (IRC) calculations using B3LYP/6-31G(D) method were performed on each TS to verify that the structure of the activated complex obtained is related to the reactants and products (Maeda *et al*., 2015). All calculations were performed in gas phase on a Gaussian 16 program suite that run on a peta-scale supercomputer (Gaussian 16, Revision C.01, 2016).

2.3. Determination of kinetic and thermodynamic parameters

The studied reaction may be summarized as a consecutive reaction with approximately 4 sub-steps (a - d) and 2 major steps, according to Equations 1 and 2:

(1)

(2)

$$G = H - TS \quad (7)$$

where H, T and S are the enthalpy, temperature (298.15 K), and entropy, respectively. The entropy, like the total energy (E) of the molecules, was obtained directly from the optimization calculation. The individual molecular enthalpy (H) was calculated as a sum of the electronic energy (total energy), zero-point energy and thermal correction to energy (Obafemi *et al*., 2018).

3.0 Results and Discussion

3.1. Choice of the theoretical model

Density functional theory (DFT) is well-known for its relatively cheaper computational cost and higher accuracy than the *ab initio* HF method (Fabiano *et al*., 2005; Tsai *et al*., 2005; Hutchison *et al*., 2005). In the same vein, the B3LYP amongst the numerous hybrid DFT functionals is the most widely used method for the prediction of geometrical properties (Fabiano *et al*., 2005; Tsai *et al*., 2005;

Hutchison *et al*., 2005). Not only that B3LYP is popular, its performance in equilibrium geometry predictions when combined with 6-31G(d) basis set has also been found to very nearly reproduce the XRD results of most organic compounds (Vijay *et al*., 2013; Mazzone *et al*., 2016). Based on this information, the ground-state molecular geometries and vibrational frequencies of the reaction components excluding CuCN and CuBr, were obtained at B3LYP/6-31G(d) level (Becke, 1993; Lee *et al*., 1988).

The mPW1PW91 functional adopted as a method of benchmarking for the optimization and frequency calculations of copper cyanide and copper halide is well known for similar systems (Golchoubian *et al*., 2015; Bayse *et al*., 2009; Kämpfe *et al*., 2015; Nitsch *et al*., 2015). The benchmarking was carried out to determine the most suitable basis set or combination of basis sets that can be used alongside the functional (mPW1PW91) for accurate prediction of CuCN geometry. The lowest total energy (-1733.12 Hartree) for CuCN was obtained with mPW1PW91/6-31g(d), hence, it was adopted as the most suitable method (Figs. S1 – S3). The reason for this choice was based on the premise that molecules would assume a most stable ground state structure at which their total energy is lowest.

3.2. Proposed reaction mechanisms and verification by DFT calculations

The changes in the geometry of the reaction components from reactants to products are presented in Fig. S10 of the supporting document. In the three proposed mechanisms, the nucleophilic substitution of Br^- by CN^- to form the activated complexes was assumed to proceed by delocalization of the π-electrons in position 4 to position 3 in the DDB (see the inset on the left in scheme 2A). This gave the way for the attack by CuCN to form *imino-copper-cyclohexa-diene carbanion* (Schemes 2A, 2B, and 3). However, in scheme 2A, it was assumed that the electron-deficient N of the cyano group takes up the Br^- at position 4, creating a space for the π-electrons to return to their original position (see the inset on the right in scheme 2A). This rearrangement was presumed to lead to the formation of the first TS structure (AC1). In AC1, the N-Br bond could break to produce the Br^- which combined with the electron-deficient Cu coming from Cu-C=N to produce the DBN and CuBr (Scheme 2A). This same cycle of electron movement and atomic rearrangement was repeated in step 2 of the reaction (iii – v) to produce the DPN and CuBr (Scheme 2A). However, the TS Berny optimized structures did not match the proposed structures for the activated complexes AC1 and AC2 in scheme 2A. This suggests that the structures of AC1 and AC2 as proposed in scheme 2A are not the true structures of the TS.

For scheme 2B, the free electrons on carbon 3 (C3) of the *cyclohexadiene* abstract the copper ion from the *imine* group on carbon 4 (C4), leaving the two electrons to resonate within the ring. Also at the same position, the Br with its two electrons migrated towards the electron-deficient imine nitrogen to give the first TS structure, AC1 (Scheme 2B). The Cu ion leaves position 3 as a leaving group with its two electrons occupying the position between C3 and C4. As the Br attached to the imine nitrogen leaves as a bromide ion, the resonating electrons complete the triple bonds between C and N in the -C=N group to make it a nitrile, thus, producing the DBN and the first CuBr (Scheme 2B). The same cycle is repeated in step 2 of the reaction leading to the formation of DPN and the second CuBr. This mechanism, like the previous one appears incorrect because the TS Berny structures obtained also did not match the proposed TS structures (AC1 and AC2). However, in Scheme 3, the structures of AC1 (ii) and AC2 (iv) proposed, were found to match the computed TS structures, which were formed by ring-closing through the Cu atom and the lone-pair electrons on the imine nitrogen, to give a triangular moiety (Fig. 4).

The intrinsic reaction path and frequency calculations confirmed that the TS structures obtained are genuine and are related to both the reactants and the proposed products. Each of the two transition states was confirmed to have no more than one imaginary frequency (Figs. S8 and S9) (Grambow *et al*., 2020).

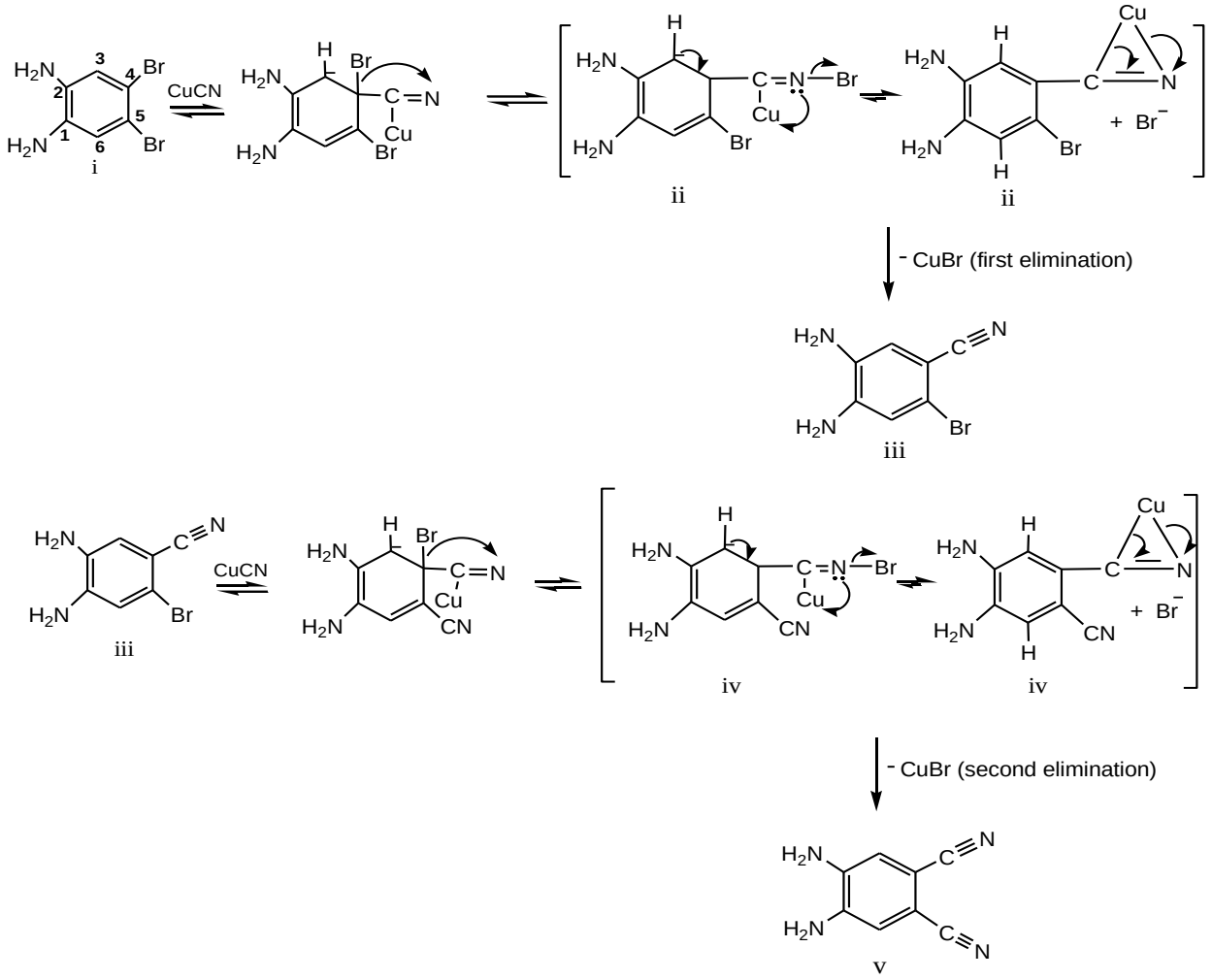

Scheme 3: The reaction mechanism that was supported by the DFT calculations.

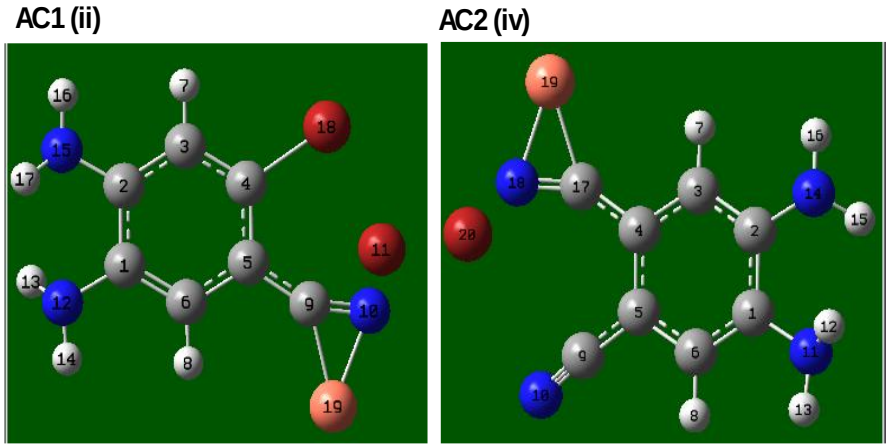

Fig. 4: Computed (Berny-optimized) first (ii) and second (iv) TS structures.

3.3 Kinetic and thermodynamic properties

The kinetic and thermodynamic data are presented in Table 1. The reaction has been assumed to kinetically proceed in two steps (Eqs. 1 and 2). The two reversible rates opposing the formation of the activated complexes in each of the two steps have been deliberately excluded in this investigation for simplicity. This is because the consideration of the rates was not based on the concentration of the reaction components, but on their E_A obtained from their total electronic energy, as proposed in Eq. 3. As shown in Table 1, the activation energy of step 2 (E_c) is higher than that of step 1 (E_a), therefore, step 2 is the rate-determining step.

Table 1: Kinetic and thermodynamic data

Kinetic data			
E_a (kJ mol^{-1})		E_c (kJ mol^{-1})	
189.0		210.6	
Thermodynamic data			
Reaction	ΔG_{reac} (kJ mol^{-1})	ΔH_{reac} (kJ mol^{-1})	ΔS_{reac} (kJ mol^{-1} K^{-1})
Step 1	-606.8	-610.7	-0.0132
Step 2	-600.1	-603.6	-0.0117

The calculated thermodynamic quantities (ΔG_{reac} and ΔH_{reac}) for the two reaction steps were used to predict the feasibility of the overall reaction. Both the ΔG_{reac} and ΔH_{reac}, for the two major steps are negative, indicating that the reaction steps are spontaneous and exothermic, respectively (Table 1). The change in entropy (ΔS_{reac}) for each of the two steps showed that the entropy decreased from reactants to products, i.e. $\Delta S_{reactants} > \Delta S_{products}$ in each step (Table 1).

The transition state thermodynamic parameters are presented in Table 2. The change in free energy of activation ($\Delta G^{\#}$) were obtained as the difference between the free energy of the activated complex and the free energy of the reactants (Levine, 1979). Similarly, the change in enthalpy of activation ($\Delta H^{\#}$) were obtained as the difference between the enthalpy of the activated complex and the enthalpy of the reactants. Both $\Delta G^{\#}$ and $\Delta H^{\#}$ were found to be positive as expected. The entropy of activation was found to be of the same magnitude and negative, for the two reaction steps, confirming that the same number of molecules are involved in the two steps. The negative sign implies that the molecularity is higher at the reactant stage compared to when in transition state for both reaction steps.

Table 2: Transition-state thermodynamic properties

Reaction	**$\Delta G^{\#}$ (kJ mol^{-1})**	**$\Delta H^{\#}$ (kJ mol^{-1})**	**$\Delta S^{\#}$ (kJ mol^{-1} K^{-1})**
Step 1	263.5	217.0	-0.156
Step 2	268.3	221.7	-0.156

4.0 Conclusion

The present study uses DFT calculations for the investigation of the formation of 4,5-diaminophthalonitrile (DPN) from the reaction between 4,5-dibromo-1,2-diaminobenzene (DDB) and copper cyanide. The study observed that the reaction mechanism involves two major steps, each proceeding through activated complexes (AC1 and AC2) and was verified to follow Scheme 3. Key findings include the identification of triangular Cu-C=N transition state structures for AC1 and AC2. Thermodynamic parameters for both steps indicate the reaction is spontaneous and exothermic. Kinetic data suggest that the second step is rate-determining, with higher activation energy compared to the first step. However, results from the DFT calculations confirmed that Scheme 3 accurately represents the mechanism for the formation of DPN from DDB and copper cyanide. The identified transition state structures (AC1 and AC2) featuring Cu-C=N frameworks provide crucial insights into the reaction pathway.

Thermodynamically, both reaction steps are favorable, supported by negative Gibbs free energy changes (ΔG_{reac}) and exothermic enthalpy changes of the reactions. The positive values of activation energies (E_a and E_c) and enthalpies of activation ($\Delta H^{\#}$) indicate that both steps proceed with an energy barrier, consistent with typical chemical reactions.

Based on the findings, further experimental validation of the proposed mechanism and thermodynamic parameters is recommended. This could include confirming the existence of the identified transition states experimentally and exploring any potential side reactions or intermediate species. Additionally, extending the computational study to consider solvent effects or alternative reaction conditions may provide a more comprehensive understanding of the reaction dynamics. Further theoretical studies could focus on optimizing reaction conditions for enhanced efficiency and yield in the synthesis of 4,5-diaminophthalonitrile, potentially addressing current synthetic limitations discussed in the literature.

5.0 References

Adegoke, O. & Nyokong, T. (2014). Unsymmetrically substituted nickel triazatetra-benzcorrole and phthalocyanine complexes: Conjugation to quantum dots and applications as fluorescent “turn on” sensors. *Journal of Fluorescence*, 24, pp. 481- 491.

Aftab, J., Farajzadeh, N., Yenilmez, H. Y., Özdemir, S., Gonca, S. and Bayir, Z. A. (2022). New phthalonitrile/metal phthalocyanine-gold nanoparticle conjugates for biological applications. *Dalton Transactions*, 51, pp. 4466 – 4476.

Albayrak, S., Farajzadeh, N., Yenilmez, H. Y., Özdemir, S., Gonca, S. and Bayir, Z. A. (2023). Fluorinated phthalocyanine/ silver nanoconjugates for multifunctional biological applications. *Chemistry and Biodiversity,* e202300389.

Baran, A., Çol, S., Karakiliç, E. and Özen, F. (2020). Photophysical, photochemical and DNA binding studies of prepared phthalocyanines. *Polyhedron*, 175: 114205.

Bayse, C. A., Brewster, T. P. & Pike, R. D. (2009). Photoluminescence of 1-D copper(I) cyanide chains: A theoretical description. *Inorganic Chemistry*, 48, pp. 174- 182.

Becke, A. D. (1993). Density-functional thermochemistry. III. The role of exact exchange. *Journal of Chemical Physics,* 98, pp. - 5653.

Camerin, M., Magaraggia, M., Soncin, M., Jori, G., Moreno, M., Chambrier, I., Cook, M. J. & Russell, D. A. (2010). The in vivo efficacy of phthalocyanine-nanoparticle conjugates for the photodynamic therapy of amelanotic melanoma. *European Journal of Cancer* 46, 10, pp. 1910 – 1918.

Demirbaş, Ü. (2020). Synthesis, characterization, photophysical and photochemical properties of novel phthalocyanines. *ChemistrySelect* , 5, 15, pp. 4530 – 4537.

de Oliveira de Siqueira, L. B., dos Santos Matos, A. P., Mattos da Silva, M. R., Pinto, S. R., Santos-Oliveira, R. & Ricci-Júnior, E. (2022). Pharmaceutical nanotechnology applied to phthalocyanines for the promotion of antimicrobial photodynamic therapy: A literature review. *Photodiagnosis and Photodynamic Therapy*, 39: 102896. https://doi.org/10.1016/j.pdpdt.2022.102896.

El-Azhary, A. A. & Suter, H. U. (1996). Comparison between optimized geometries and vibrational frequencies calculated by the DFT methods, *Journal of Physical Chemistry*, 100, pp. 15056-15063.

Fabiano, E., Sala, F. D., Cingoland, R., Weimer, M. & Görling, A. (2005).

Theoretical study of singlet and triplet excitation energies in oligothiophenes, *Journal of Physical Chemistry*, *A*, 109, pp. 3078 – 3085.

Farajzadeh, N., Aftab, J., Yenilmez, H. Y., Özdemir, S., Gonca, S. & Bayir, Z. A. (2022). The design and synthesis of metallophthalocyanine-gold nanoparticle hybrids as biological agents. *New Journal of Chemistry*, 46, pp. 5374 – 5384.

Farahmand, S., Ayazi-Nasrabadi, R. & Zolfigol, M. A. (2023). Amino-cobalt(II) phthalocyanine supported on silica chloride as an efficient and reusable heterogeneous photocatalyst for oxidation of alcohols. *Tetrahedron Letters*, 118: 154403. https://doi.org/10.1016/j.tetlet.2023.154403.

Gamelas, S. R. D., Tomé, J. P. C., Tomé, A. C. & Lourenço, L. M. O. (2023). Advances in photocatalytic degradation of organic pollutants in wastewaters: harnessing the power of phthalocyanine and phthalocyanine-containing materials. *RSC Advances* 13, pp. 33957-– 33993.

Gaussian 16, Revision C.01, Frisch, M. J., Trucks, G. W., Schlegel, H. B., Scuseria, G. E., Robb, M. A., Cheeseman, J. R., Scalmani, G., Barone, V., Petersson, G. A., Nakatsuji, H., Li, X., Caricato, M., Marenich, A. V., Bloino, J., Janesko, B. G., Gomperts, R., Mennucci, B., Hratchian, H. P., Ortiz, J. V., Izmaylov, A. F., Sonnenberg, J. L., Williams-Young, D., Ding, F., Lipparini, F., Egidi, F., Goings, J., Peng, B., Petrone, A., Henderson, T., Ranasinghe, D., Zakrzewski, V. G., Gao, J., Rega, N., Zheng, G., Liang, W., Hada, M., Ehara, M., Toyota, K., Fukuda, R., Hasegawa, J., Ishida, M., Nakajima, T., Honda, Y., Kitao, O., Nakai, H., Vreven, T., Throssell, K., Montgomery, J. A. Jr, Peralta, J. E., Ogliaro, F., Bearpark, M. J., Heyd, J. J., Brothers, E. N., Kudin, K. N., Staroverov, V. N., Keith, T. A., Kobayashi, R., Normand, J., Raghavachari, K., Rendell, A. P., Burant, J. C., Iyengar, S. S., Tomasi, J., Cossi, M., Millam, J. M., Klene, M., Adamo, C., Cammi, R., Ochterski, J. W., Martin, R. L., Morokuma, K., Farkas, O., Foresman, J. B. and Fox, D. J. (2019) Gaussian, Inc., Wallingford CT.

Golchoubian, H., Moayyedi, G. & Reisi, N. (2015). Halochromism, ionochromism, -solvatochromism and density functional study of a synthesized copper(II) complex containing hemilabile amide derivative ligand. *Spectrochimica Acta A Molecular Biomolecular Spectroscopyopy*, 138, pp. 913 -924.

Grambow, C. A., Pattanaik, L. & Green, W. H. (2020). Reactants, products, and transition states of elementary chemical reactions based on quantum chemistry. *Science Data* 7: 137, https://doi.org/10.1038/s41597-020-0460-4.

Gregory P. (2000). Industrial applications of phthalocyanines. *Journal of Porphyrins and Phthalocyanines*, 4, 4, pp. 432 – 437.

Gvozdev, D. A., Solovchenko, A. E., Martynov, A. G., Yagodin, A. V., Strakhovskaya, M. G., Gorbunova, Y. G. & Maksimov, E. G. (2022). Fluorescence quenching of carboxy-substituted phthallocyanines conjugated with nanoparticles under high stoichiometric ratios. Photonics 9, 9, 668. 10.3390/photonics9090668.

Guney, G. & Gorduk, S. (2023). Photophysical and photochemical studies on non-peripherally and peripherally Ga(III) chloro phthalocyanines in different solvents. *Journal of Organometallic Chemistry*, 999: 122813.

Hutchison, G. R., Ratner, M. A. & Marks, T. J. (2005). Hopping transport in conductive heterocyclic oligomers: Reorganization energies and substituent effects, *Journal*

of American Chemical Society, 127, pp. 2339- 2350.

Idowu, M. & Nyokong, T. (2012). Photophysical behavior of fluorescent nanocomposites of phthaloyanine linked to quantum dots and magnetic nanoparticles. International Journal of Nanoscience 11(2): 1250018.

Kahriman, N., Ünver, Y., Akçay, H. T., Gülmez, A. D., Durmuş, M. & Değirmencioğlu, Î. (2020). Photophysical and photochemical study on novel axially chalcone substituted silicon (IV) phthalocyanines. *Journal of Molecular Structure*, 1200, : 127132(1-10).

Kämpfe, A., Brendler, E., Kroke, E. & Wagler, J. (2015). Tp*Cu(I)-CN-SiL_2-NC-Cu(I)Tp* - a hexacoordinate Si-complex as connector for redox active metals *via* π-conjugated ligands, *Dalton Transactions*, 44, pp. 4744 - 4750.

Korkmaz, E., Ahmetali, E., Atmaca, G. Y., Karaoğlu, H. P., Erdoğmuş, A. & Koçak, M. B. (2020). Investigation of photophysical and photochemical properties of phthalocyanines bearing fluorinated groups. *Monatshefte für Chemie*, 151, pp. 181-190.

Kumar, A., Prajapati, P. K., Aathira, M. S., Bansiwal, A., Boukherroub, R. & Jain, S. L. (2019). Highly improved photoreduction of carbon dioxide to methanol using cobalt phthalocyanine grafted to graphitic carbon nitride as photocatalyst under visible light irradiation. *Journal of Colloid Interface Science*, 543, pp. 201- 213.

Lee, C., Yang, W. & Parr, R. G. (1988). Development of the colle-salvetti correlation-energy formula into a functional of the electron density. *Physical Review B*, 37, pp. 785 – 789.

Levine, R. D. (1979). Free energy of activation. Definition, properties, and dependent variables with special reference to "linear" free energy relation, *Journal of Physical Chemistry*, 83, 1, pp. 159- 170.

Lo, P-C., Rodríguez-Morgade, M. S., Pandey, R. K., Ng, D. K. P., Torres, T. & Dumoulin, F. (2020). The unique features and promises of phthalocyanines as advanced photosensitizers for photodynamic therapy of cancer. *Chemical Society Reviews*, 49, pp. 1041 – 1056.

Madhuri, K. P. and John, N. S. (2022). Chapter 18 – Metal phthalocyanines and their composites with carbon nanostructures for applications in energy generation storage, in: Design, fabrication, and characterization of multifunctional nanomaterials. *Micro and Nanotechnologies,* 401 – 448.

Maeda, S., Harabuchi, Y., Ono, Y., Taketsugu, T. & Morokuma, K. (2015). Intrinsic reaction coordinate: Calculation, bifurcation, and automated search. *International Journal of Quantum Chemical,* 115, 5, pp. 258 – 269.

Mafukidze, D. M., Sindello, A. & Nyokong T. (2019). Spectroscopic characterization and photodynamic antimicrobial chemotherapy of phthalocyanine-silver triangular nanoprism conjugates when supported on asymmetric polymer membranes. *Spectrochimica Acta Part A Molecular and Biomolecular Spectroscopy*, 219, pp..333 – 345.

Matlou, G. G. & Nyokong, T. (2020). Photophysico-chemical properties and photoinactivation of *Staphylococcus Aureus* using zinc phthalocyanines linked silver nanoparticles conjugates. *Dyes and Pigments*, 108237, (1 – 11).

Mazzone, G., Alberto, M. E., De Simone, B. C., Marino, T. & Russo, N. (2016). Can Expanded Bacteriochlorins act as photosensitizers in photodynamic Therapy? Good news from density functional theory computations. *Molecules*, 21: 288.

Ndebele, N. & Nyokong, T. (2023). The use of carbon-based nanomaterials conjugated to
cobalt phthalocyanine complex in the electrochemical detection of nitrite. *Diamond and Related Materials,* 132, 109672.

Nitsch, J., Kleeberg, C., Fröhlich, R. & Steffen, A. (2015). Luminescent copper(I) halide andpseudohalide phenanthroline complexes revisited: simple structures, complicated, excited state behavior, *Dalton Transactions*, 44, pp. 6944 - 6960.

Obafemi, C. A., Fadare, O. A., Jasinski, J. P., Millikan, S. P., Obuotor, E. M., Iwalewa, E. O., Famuyiwa, S. O., Sanusi, K., Yilmaz, Y. & Ceylan, Ü. (2018). Microwave-assisted synthesis, structural characterization, DFT studies, antibacterial and antioxidant activity of 2-methyl-4-oxo-1,2,3,4-zetrahydroquin - azoline-2-carboxylic acid. *Journal of Molecular Structure* 1155, pp. 610 – 622.

Pan, K., Tang, X., Qu, G., Tang, H., Wei, K. & Lv, J. (2023). Mesoporous silica/iron phthalocyanine light-driven nanomaterials for efficient removal of Pb^{2+} ions from wastewater. *Applied Nano Materials*, 6, 14, pp. 12816 – 12827.

Salzner, U. (2010). Modeling photoelectron spectra of conjugated oligomers with time-dependent density functional theory, *Journal of Physical Chemistry*, *A*, 114, pp. 10997-11007.

Sánchez, C. O. & Rivas, B. L. (2002). Poly(1,2-diaminobenzene) and poly(1,3-Diamino benzene): synthesis, characterization, and properties. *Journal of Applied Polymer Science*, 85, pp. 2564 – 2572.

Sanusi, K., Amuhaya, E. K. & Nyokong, T. (2014). Enhanced optical limiting behavior of an indium phthalocyanine-single-walled carbon nanotube composite: an investigation of the effects of solvents. *Journal of Physical Chemistry C* 118, pp. 7057-7069.

Sanusi, K., Antunes, E. & Nyokong, T. (2014). Optical nonlinearities in non-peripherally substituted pyridyloxy phthalocyanines: a combined effect of symmetry, ring-strain and demetallation. *Dalton Transactions*, 43, 999-1010.

Sanusi, K., Ceylan, Ü., Yilmaz, Y. & George, R. C. (2020). A DFT/TD-DFT study on the possible replacement of Ru(II) with Fe(II) in phthalocyanine-based dye-sensitized solar cells. *Structural Chemistry*, 31, pp. 2301 – 2311.

Sanusi, K., Khene, S. & Nyokong, T. (2014). Enhanced optical limiting performance in phthalocyanine-quantum dot nanocomposites by free-carrier absorption mechanism. *Optical Materials*, 37, pp. 572-582.

Sanusi, K. & Nyokong, T. (2014). Indium phthalocyanine-CdSe/ZnS quantum dots nanocomposites showing size dependent and near ideal optical limiting behavior. *Optical Materials*, 38, pp. 17-23.

Sanusi, K., Stone, J. M. & Nyokong, T. (2015). Nonlinear optical behavior of indium-phthalocyanine tethered to magnetite or silica nanoparticles. *New J. Chem*. 39, pp. 1665 – 1677.

Sayyah, S. M., Khaliel, A. B., Aboud, A. A. & Mohamed, S. M. (2014). Chemical polymerization kinetics of poly-o-phenylenediamine and characterization of the obtained polymer in aqueous hydrochloric acid solution using $K_2Cr_2O_7$ as oxidizing agent. *International Journal of Polymer Science*, 2014, pp. 1-16. http://dx.doi.org/10.1155/2014/520910.

Siddle, J. S., Ward, R. M., Collings, J. C., Rutter, S. R., Porrès, L., Applegarth, L., Beeby, A., Batsanov, A. S., Thompson, A. L., Howard, J. A. K., Boucekkine, A., Costuas, K., Halet, J. F. & Marder, T. B. (2007). Synthesis, photophysics and molecular structures of luminescent 2,5-bis(phenylethynyl)thiophenes (BPETs), *New Journal of Chemistry*, 31: 841-851.

Song, P. and Ma, F. (2010). Tunable electronic structures and optical properties of fluorenone-based molecular materials by heteroatoms. *Journal of Physical Chemistry A* 114, pp. 2230-2234.

Subhan, M. A., Perveen, F., Filipczak, N., Yalamarty, S. S. K. & Torchilin, V. P. (2023). Approaches to improve EPR-based drug delivery for cancer therapy and diagnosis. *Journal of Personalized Medicine*, 13, 389. https://doi.org/10.3390/jpm13030389.

Suleimanov, Y. V. & Green, W. H. (2015). Automated discovery of elementary chemical reaction steps using freezing string and Berny optimization methods. *Journal of Chemical Theory and Computation*, 11, 9, pp. 4248 – 4259.

Tayfuroğlu, Ö., Kiliçarslan, F. A., Atmaca, G. Y. & Erdoğmuş, A. (2018). Synthesis,

characterization, of new phthalocyanines and investigation of photophysical, photochemical properties and theoretical studies. *Journal of Porphyrins and Phthalocyanines*, 22: 250 - 265.

Tsai, F. -C., Chang, C. -C., Liu, C. -L., Chen, W. C. & Jenekhe, S. A. (2005). New thiophene-linked conjugated poly (azomethines): Theoretical electronic structure, synthesis, and properties. *Macromolecules*, 38, pp. 1958-1966.

Tunç, G., Güzel, E., Şişman, İ., Ahsen, V., árdenas-Jirón, G. & Gürek, A. G. (2019). Effect of new asymmetrical Zn(II) phthalocyanines on the photovoltaic performance of a dye-sensitized solar cell. *New Journal of Chemistry*, 43, pp. 14390 – 14401.

Vijay, D., Varathan, E. & Subramanian, V. (2013). Theoretical design of core modified (oxa and thia) porphyrin based organic dyes with bridging thiophene linkers. *Journal of Materials Chemistry A*, 1, pp. 4358-4369.

Yang, S., Yu, Y., Gao, X., Zhang, Z. & Wang, F. (2021). Recent advances in electrocatalysis with phthalocyanine. *Chemical Society Reviews*, 50, pp. 12985-13011.

Yüksel, F., Gürek, A. G., Lebrun, C. & Ahsen, V. (2005). Synthesis and solvent effects on the spectroscopic properties of octatosylamido phthalocyanines. *New Journal of Chemistry*, 29, pp. 726 – 732.

Yüksel, F., Tuncel, S. & Ahsen, V. (2008). Synthesis and characterizations of *peripheral* octa-amino and octa-amidophthalocyanines. *Journal of Porphyrins and Phthalocyanines*, 12, pp. 123 – 130.

Yüzeroğlu, M., Karaoğlan, G. K., Köse, G. G. & Erdoğmuş, A. (2021). Synthesis of new zinc phthalocyanines including Schiff base and halogen; photophysical, photochemical, and fluorescence quenching studies. *Journal of Molecular Structure* 1238 (2021) 130423(1 – 10).

Zhang, X-F., Li, X., Niu, L., Sun, L. & Liu, L. (2009). Charge Transfer Photophysics of Tetra(α-amino) Zinc Phthalocyanine. *Journal of Fluorescence*, 19, pp. 947–954.

Zhang, X, F. & Xu, H. (1994). Synthesis and photophysical properties of substituted zinc phthalocyanines. *Chemical Research in Chinese Universities*, 15, pp. 917 – 921.

Zi, Y., Yang, K., He, J., Wu, Z., Liu, J. & Zhang, W. (2022). Strategies to enhance drug delivery to solid tumors by harnessing the EPR effects and alternative targeting mechanisms. *Advanced Drug Deliv*ery 188: 114449.

Acknowledgement

The author is grateful to Dr. P. B. Khoza and the management of the Centre for High-Performance Computing (CHPC), South Africa, for access to their central supercomputing cluster.

Compliance with Ethical Standards
Declaration
Ethical Approval

Not Applicable

Competing interests

The authors declare that they have no known competing financial interests or personal relationships that could have appeared to influence the work reported in this paper.

Funding

The No funding.

Availability of data and materials

Data would be made available on request.

Authors' contributions

Conception, investigation, data analysis and interpretation, manuscript writing and editing were done by KS.